THE JOURNAL OF BIOLOGICAL CHEMISTRY
Vol. 274, No. 50, Issue of December 10, pp. 35768–35776, 1999
Printed in U.S.A.

The Motif D Loop of Human Immunodeficiency Virus Type 1 Reverse Transcriptase Is Critical for Nucleoside 5′-Triphosphate Selectivity*

(Received for publication, June 17, 1999, and in revised form, August 2, 1999)

Bruno Canard‡§, Kajal Chowdhury§¶, Robert Sarfati‖, Sylvie Doublié¶, and Charles C. Richardson¶‡‡**

From the ‡Centre National de la Recherche Scientifique, Ecole Supérieure d'Ingénieurs de Luminy, Architecture et Fonction des Macromolécules Biologiques, 163 avenue de Luminy, 13288 Marseille cedex 9, France, the ¶Department of Biological Chemistry and Molecular Pharmacology, Harvard Medical School, Boston, Massachusetts 02115, and the ‖Institut Pasteur, 28 rue du Docteur Roux, 75724 Paris cedex 15, France

Human immunodeficiency virus type 1 reverse transcriptase (RT) has limited homology with DNA and RNA polymerases. The conserved Lys-220 of motif D is a signature of RNA-dependent polymerases. Motif D is located in the "palm" domain and forms a small loop from Thr-215 to Lys-223. This loop is absent from the polymerase I family of DNA-dependent polymerases. Analysis of RT structures in comparison with other polymerases reveals that the motif D loop has the potential to undergo a conformational change upon binding a nucleotide. We find that amino acid changes in motif D affect the interaction of RT with the incoming nucleotide. A chimeric RT in which the loop of motif D is substituted by the corresponding amino acid segment from *Taq* DNA polymerase lacking this loop has a decreased affinity for incoming nucleotides. We have also constructed a mutant RT where the conserved lysine at position 220 within the motif D is substituted with glutamine. Both RT(K220Q) and the chimeric RT are resistant *in vitro* to 3′-deoxy 3′-azidothymidine 5′-triphosphate (AZTTP). These results suggest that motif D is interacting with the incoming nucleotide and a determinant of the sensitivity of reverse transcriptases to AZTTP. We do not observe any interaction of motif D with the template primer.

Reverse transcriptase (RT)[1] catalyzes the synthesis of a double-stranded DNA molecule from the human immunodeficiency virus (HIV) (+) single-stranded RNA genome. This DNA polymerase, encoded by the viral *pol* gene, is one of the current targets of inhibitors aimed at controlling the replication of this pathogen. The clinical importance of HIV has led to extensive studies of its RT. RT shares structural similarities with both DNA and RNA polymerases. Primary sequence homology with other polymerases has been useful in identifying both catalytically important amino acids and functional domains (1, 2). The comparison of the crystal structure of RT with other polymerases whose structure is available suggests that all polymerases have a common mechanism for nucleotide polymerization (3, 4). The overall structure of these enzymes can be compared with an open right hand holding the 3′-end of the primer annealed to its template in the "palm" between the "thumb" and "fingers" domains (5).

Several conserved signature sequences, designated from A to E, have been identified using amino acid sequence alignments (6). Motifs A and C, present in all polymerases, are located in the palm domain and contain conserved acidic amino acids essential for catalysis (1, 2). Two aspartic acid residues that coordinate a magnesium ion are part of the polymerase active site. Motifs A and C are present in all nucleic acid polymerases (1, 2). The function of motif B in the fingers domain has been defined both structurally and biochemically for DNA polymerases from the Pol I family: *Thermus aquaticus* (*Taq*) DNA polymerase (7), Klenow fragment of *Escherichia coli* DNA polymerase I (8), and the DNA polymerase of bacteriophage T7 (9). Motif B consists a α-helix designated also as "helix O" in the Klenow fragment structure (5). Based on the crystal structure of T7 DNA polymerase in complex with a template primer and a nucleoside 5′-triphosphate, it appears that upon binding to DNA and the correct nucleotide the fingers domain rotates inwards toward the polymerase active site. This conformational change brings conserved residues of helix O in contact with the incoming nucleotide (9). RT has a domain of two anti-parallel β-strands named β3 and β4 spatially equivalent to helix O of motif B. Indirect evidence suggests that this domain has the same role in nucleotide binding as motif B. Amino acid changes in this domain lead to resistance to nucleotide analogues in viral strains carrying these mutations (10), and an antibody designed to recognize an epitope located in motif B acts as a competitive inhibitor for nucleotides during polymerization (11). However, another role for the β3/β4 strands was proposed in which the β3/β4 strands would make contacts with the single-stranded template instead of the incoming nucleotide (12). In this model, the single-stranded template would pass through the cleft formed by the fingers, palm, and thumb domains. During the course of our study, the crystal structure of a ternary complex of RT-DNA-nucleotide was determined at 3.2 Å resolution (13). This structure is presented in Fig. 1. A large cleft, which accommodates the template primer, is a common feature of all polymerases whose structure is

* This work was supported in part by Grant AI-06045 from the National Institutes of Health, by Grant DE-GF88ER60688 from the Department of Energy, and by the Fonds pour la Recherche Médicale (Sidaction). The costs of publication of this article were defrayed in part by the payment of page charges. This article must therefore be hereby marked "*advertisement*" in accordance with 18 U.S.C. Section 1734 solely to indicate this fact.

§ These authors contributed equally to this work.

** Present address: Dept. of Microbiology & Molecular Genetics, Markey Center for Molecular Genetics, University of Vermont, Burlington, VT 05405.

‡‡ To whom correspondence should be addressed. Tel.: 617-432-1864; Fax: 617-432-3362; E-mail: ccr@hms.harvard.edu.

[1] The abbreviations used are: RT, reverse transcriptase; HIV, human immunodeficiency virus, AZT, 3′-azido 3′-deoxythymidine; AZTMP, 3′-azido 3′-deoxythymidine 5′-monophosphate; AZTTP, 3′-azido 3′-deoxythymidine 5′-triphosphate; dNTP, 3′-deoxynucleoside 5′-triphosphate; ddNTP, 2′-3′-dideoxynucleoside 5′-triphosphate; Pol I, polymerase I.

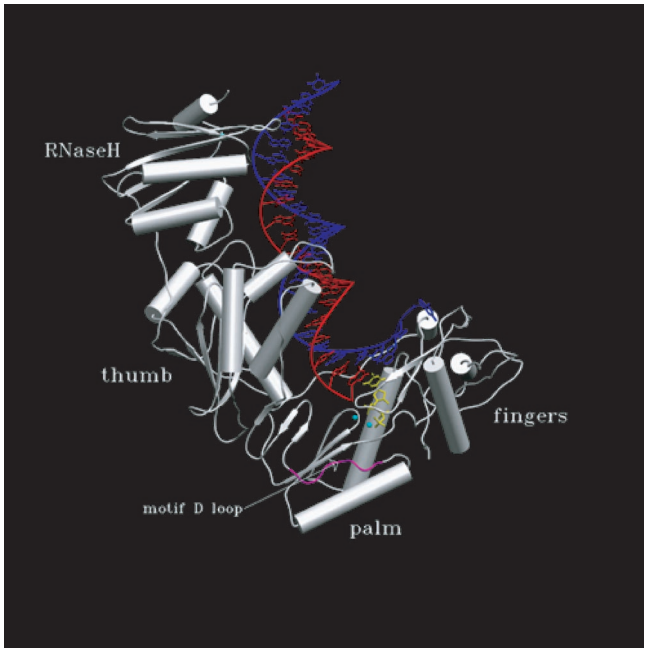

FIG. 1. **Crystal structure of RT in complex with a double-stranded DNA template primer and a nucleotide.** The atomic coordinates of Huang *et al*. (13) were used to visualize the complex using the program SETOR. The p66 subunit of HIV-1 RT is shown in *gray*. The template strand is represented in *blue*, the primer strand is in *red*, the dTTP nucleotide is in *yellow*, and the two Mg^{2+} ions are in *cyan*. Motif D loop is shown in *purple*. The different subdomains of the p66 subunit of HIV-1 RT are indicated in the figure. Duplex DNA bound by RT is oriented approximately perpendicular to the plane of the figure, and the 3′-end of the primer points toward the reader.

known. Like T7 and *Taq* DNA polymerases, the crystal structure of the RT ternary complex shows that the single-stranded template does not pass through the crevice between the fingers and thumb, but instead lies on the surface of the finger as the result of a sharp kink in the template strand (9, 13, and 14). The last nucleotide at the 3′-end of the primer stacks against the incoming nucleotide, which in turn stacks against the fingers domain (Fig. 1). This domain is helix O of motif B in T7 and *Taq* DNA polymerases (9, 14) or the β3 strand in RT (Fig. 1 and Ref. 13). Consequently, despite their structural differences, both motif B and β3/β4 strands are likely to interact with the nucleotide before the catalytic step.

In addition to these three motifs, RNA-directed polymerases contain in their palm region an additional motif, motif D, that is not found in other DNA polymerases (6). Motif D is located in the palm domain and forms a small loop from Thr-215 to Lys-223 of HIV-1 RT. The role of motif D is unknown. Because motif D is unique to RNA-directed polymerases, one possible role would be that it confers specificity for the RNA template (6, 15). However, both its location in the palm domain and the fact that several amino acid changes such as T215(F/Y) and K219Q that lead to nucleoside analogue resistance are found in this motif of RT suggest otherwise (10). In this paper, we show that motif D participates in nucleotide selection and catalysis and not in template specificity.

EXPERIMENTAL PROCEDURES

Gene Constructions—The RT gene cloned into a M13 bacteriophage vector to give mpRT4 has been described (16). mpRT4 single-stranded DNA was used to construct a RT gene carrying five additional unique restriction sites (*NruI*, *Sal*I, *Hpa*I, *Sac*I, and *Eco*47III) that do not alter the wild-type amino acid sequence. Using the first C of Pro-1 codon of the RT gene as a reference, the nucleotide position of the first base of the recognition sequence of these sites are 182, 223, 639, 897, and 1657 for *NruI*, *Sal*I, *Hpa*I, *Sac*I, and *Eco*47III, respectively. These silent sites correspond to amino acids 62, 73, 214, 233, and 553, respectively. This gene expressing wild-type RT was subcloned into the vector pTrc99A (Amersham Pharmacia Biotech) to yield p66RT1 using the same strategy as described (17). A synthetic, phosphorylated double-stranded oligonucleotide carrying six histidine codons immediately before the stop codon was ligated between the dephosphorylated *Eco*47III and *Hin*dIII sites of p66RT1 to yield p66RT2. The *Hpa*I site present in the vector backbone at nucleotide position 3909 using the pTrc99A sequence as the reference was eliminated by mutagenesis to yield p66RT7. To introduce mutations between residue 62 and 73, p66RT7 was digested with *NruI* and *Sal*I, dephosphorylated, and ligated to a double-stranded, phosphorylated synthetic oligonucleotide carrying the desired mutated codon. The same strategy was used to introduce mutations within the *Hpa*I-*Sac*I DNA fragment corresponding to peptide fragment Leu-214 to Lys-233. All plasmid constructions containing RT genes were verified by restriction enzyme analysis and DNA sequencing.

Gene Expression and Enzyme Purification— E. coli XL1-Blue (Stratagene) was used to express RT genes. In some instances, RT without histidine extension was purified as described (17). Recombinant wild-type and mutant HIV-1 RT were overproduced in *E. coli* and purified as p66/p66 homodimers using conventional chromatographic methods (17) or using metal chelate chromatography (Qiagen). All preparations of RT were >95% pure as determined by SDS-gel electrophoresis and Coomassie Blue staining. The purified wild-type enzyme had a specific activity from 8000 to 9500 units/mg protein. One unit of enzyme catalyzes the incorporation of 1 nmol of DE-81 absorbable dTMP in 10 min at 37 °C using poly(rA)·oligo$(dT)_{19}$ as a template primer. RT concentrations were determined using a standard colorimetric assay and spectrophotometrically using the extinction coefficients of Kati *et al.* (18).

Reagents—Oligonucleotides were obtained from Oligos Etc. Inc. Oligonucleotides were 5′-^{32}P-labeled using phosphatase-free bacteriophage T4 polynucleotide kinase purified and provided by S. Tabor (Harvard Medical School). All ^{32}P-labeled nucleotides were from Amersham Pharmacia Biotech. 3′-Deoxy- and 2′3′-dideoxynucleoside 5′-triphosphates (ddNTPs and dNTPs) were from Amersham Pharmacia Biotech. 3′-Azido-3′-deoxythymidine 5′-triphosphate (AZTTP) was synthesized and purified at the Institut Pasteur (Paris, France). Synthesis of DNA primers containing a *p*-azidophenacyl photo-reactive probe has been described (19).

DNA-Protein Cross-Linking Assays Using Photoprobe-coupled Oligonucleotide—The affinity of RT for its template primer was analyzed by UV cross-linking of RT to a labeled DNA primer. The *p*-azidophenacyl modified 21-mer primer was labeled with ^{32}P at the 5′-end and annealed to a 31-mer DNA as described (19). RT (250 nM) was mixed (1:1 v/v) with an equimolar amount of 5′-^{32}P template primer on parafilm laid on a flat, ice-cold surface in a 10-μl final volume of 10% glycerol, 5 μg/ml bovine serum albumin, 5 mM $MgCl_2$, 25 mM potassium phosphate buffer, pH 7.4, 1 mM dithiothreitol, 50 mM KCl. The mixture was irradiated (λ = 365 nm) with a two-bulb 15-W UV lamp at a distance of 2 cm to yield an UV irradiation dose of 0.1–0.2 W/cm^2. The mixture was heated in loading buffer containing 80% formamide, 4% SDS, 1 mM β-mercaptoethanol at 95 °C for 3 min and loaded onto a SDS-polyacrylamide gel containing 7 M urea. Gels were covered with cellophane wrap, radioactive signals were measured using a Fuji imaging apparatus, and the gel was exposed to x-ray films.

Comparison of Equilibrium Dissociation Constants (K_d) for Template Primer and RT—The efficiency of cross-linking of RT to the photoprobe-coupled labeled primer depends on the affinity of RT for the template primer. The affinity constant K_d of wild-type RT for its template primer is known (17). Comparison of cross-linking efficiencies of variant RTs relative to that of wild-type RT was used to determine the K_d of variant RTs for template primer. To determine how the concentration of the complex made of RT cross-linked to template primer [ED] varied with K_d of RT for template primer, the former complex [ED] was plotted against K_d using Equation 5, derived as follows.

$$K_d = [E][D]/[ED] \quad \text{(Eq. 1)}$$

$$[E_0] = [E] + [ED] \quad \text{(Eq. 2)}$$

$$[D_0] = [D] + [ED] \quad \text{(Eq. 3)}$$

where $[E_0]$, $[D_0]$, [E], [D], [ED], and K_d are initial RT, initial template primer, free RT, free template primer, free RT-template primer complex concentrations, and the equilibrium constant K_d of RT for the template primer, respectively. Combining Equations 1–3 yields the following.

$$-[D]^2 + [D]([D_0] - [E_0] - K_d) - K_d[D_0] = 0 \quad \text{(Eq. 4)}$$

In our assay, $[D_0] = [E_0] = 250$ nM. Solving for [D] and using Equation 3 yields the following.

$$[ED] = [D_0] - [K_d \pm ((-K_d)^2 + 1000 \cdot K_d)^{0.5}]/-2 \quad \text{(Eq. 5)}$$

Plotting [ED] as a function of chosen values of K_d models how the RT-template primer cross-linked complex [ED] varies according to the affinity constant K_d of a given variant RT for its template primer. Using $K_d = 5$ nM for wild-type RT (17) and Equation 5, the difference between two cross-linked RT-primer complexes as seen on a gel indicates how different their K_d values are. In other words, for any variant RT the percentage of variation of [ED] relative to wild-type RT seen as a cross-linked species on a gel and Equation 5 can be used to calculate K_d of the variant RT. Data analysis was performed using nonlinear regression and the Kaleidagraph 3.0 software for MacIntosh (Abelbeck Software, Inc).

Determination of Equilibrium Dissociation Constants for Template Primer and RT—K_d values were also determined using a kinetic assay and poly(rA)·oligo(dT)$_{19}$ as a template primer system as described Huber *et al.* (25). DNA synthesis from a preformed complex of polymerase and template primer is limited to a single processive cycle. Varying concentrations of poly(rA)·oligo(dT)$_{19}$ ranging from 1 to 120 nM were incubated with three different concentrations of RT, 10, 5, or 2.5 nM enzyme in a 50-μl reaction mixture containing 50 mM Tris-HCl, pH8, 50 mM KCl, 10 mM $MgCl_2$, 0.05% Triton X-100 on ice for 1 min. The reaction was initiated by adding a mixture of 150 μM dTTP and 500 nM poly(rC).(dG)$_{20}$ to serve as a trap. The reaction was incubated at 37 °C for 10 min and terminated by the addition 10 μl of 0.5 M EDTA. Aliquots were spotted onto DE-81 filter papers. The filter papers were washed three times with 0.3 M ammonium formate and once with 95% ethanol. The radioactivity bound to the filters was determined by liquid scintillation counting. The affinity for the template primer was expressed as an average of the values obtained from an Eadie-Hofstee plot .

Processivity Assay—Processivity of nucleotide polymerization was measured using a 5′-^{32}P-labeled oligo(dT)$_{19}$ primer annealed to poly(rA). The template average length was 612 nucleotides and was annealed to primer using a 1:1 molar ratio calculated using nucleotide concentration. The template primer (10 nM) was incubated with RT (20 nM) for less than 2 min in RT buffer (50 mM Tris-HCl, pH 8.0, 50 mM KCl, 10 mM $MgCl_2$, 0.05% Triton X-100) at 25 °C. The reaction was initiated by the addition of 1 mM dTTP in the absence or presence of 2 μg/μl heparin to serve as a trap and incubated at 25 °C. After 1 and 5 min, an aliquot of the reaction was quenched with an equal volume of gel loading buffer made of 90% formamide, 0.1% bromphenol blue, 0.1% xylene cyanol, and 10 mM EDTA. The optimum trap concentration was found to be 2 μg/μl of heparin for wild-type RT and the two mutant HIV-1 RT (data not shown). Electrophoretic analysis was performed on a 12% denaturing polyacrylamide gel, and the gel was analyzed as described above.

Reverse Transcriptase Assays—RT activity was determined by monitoring the formation of radioactively labeled nucleic acid product absorbed onto DE-81 ion exchange paper discs. Reactions were carried out in RT buffer in the presence of 50 μg/μl poly(rA)·oligo(dT)$_{19}$, poly(rC)·oligo(dG)$_{19}$, or poly(rU)·oligo(dA)$_{21}$ in conjunction with 100 μM of [^{3}H]dTTP (36 μCi/μmol), 100 μM [α-^{32}P]dGTP (0.2 μCi/μl), or 100 μM [α-^{32}P]dATP (0.2 μCi/μl), respectively. After addition of RT, aliquots were withdrawn at several time points and spotted onto DE-81 paper discs. To determine the K_m for dNTP, template primers were kept at a saturating concentration of 200 nM, and the concentrations of the corresponding dNTP were varied from 2 μM to 1 mM. The RT concentration was 20 nM. Filter paper discs were washed three times for 10 min in 0.3 M ammonium formate, pH 8.0, washed two times in ethanol, and dried. The radioactivity bound to the filters was determined by liquid scintillation counting.

Nucleotide Analogue Inhibition Assays—For nucleotide analogue inhibition assays, poly(rA)·oligo(dT)$_{19}$ was used as the template primer. AZTTP is a competitive inhibitor of dTTP (26). To determine K_i(AZTTP), the dTTP concentration was kept constant and equal to K_m(dTTP) determined as described above. AZTTP concentration was varied, and K_i was determined as being equal to the concentration of AZTTP producing 50% inhibition of the polymerization reaction. To compare RT variants under the same experimental conditions, the concentration of dTTP was kept constant at 100 μM, while concentrations of either AZTTP or ddTTP were varied as indicated. Polymerase activity was normalized using the uninhibited reaction as a reference. Using wild-type RT, the concentration of AZTTP and ddTTP producing a 50% inhibition of polymerase activity (IC_{50}) was 0.1 and 0.3 μM for AZTTP and ddTTP, respectively. For a given RT, discrimination of the analogue was calculated as the ratio of measured IC_{50} to the IC_{50} of wild-type RT.

The degree of AZTTP and ddTTP discrimination was also examined by gel analysis of primer extension products (20). The reaction mixture containing 50 mM Tris-HCl, pH 8.0, 50 mM KCl, 10 mM $MgCl_2$, 0.05% Triton X-100, 1 mM dTTP, and 100 nM poly(rA)[chemo]5′-^{32}P·oligo(dT)$_{19}$ template primer was incubated with 50 nM enzyme either in the presence or absence of 100 μM AZTTP or ddTTP as indicated. The reaction (10 μl) was initiated by the addition of the enzyme and terminated by the addition of an equal volume of stop solution. The products were analyzed as described above.

Three-dimensional Computer Modeling of RT—The coordinates of RT were obtained from the Brookhaven Protein Data Base. Their accession numbers are indicated in the text and figure legends. The crystal structure models were displayed using INSIGHT II, SETOR, and the TURBO graphics programs (21). Structural alignment was performed using the RIGID option of TURBO.

RESULTS

We have investigated the role of motif D of HIV-1 RT in reverse transcription and DNA-dependent nucleotide polymerization. On one hand, this motif is found specifically in RNA-dependent DNA and RNA polymerases as opposed to DNA-dependent polymerases, suggesting a role in template specificity (6). On the other hand, motif D is located in the palm domain of RT away from the template track (13). Furthermore, two (T215(F/Y) and K219Q) out of five clinically relevant amino acid changes (M41L, D67N, K70R, T215(F/Y), and K219Q) involved in AZT resistance are located in this motif, suggesting a role in nucleotide selection (10, 22). It was thus of interest to determine whether amino acid changes in motif D would affect template specificity or interaction with the nucleotide during DNA polymerization. Therefore, we generated RT variants altered in motif D and characterized their template primer binding properties as well as their kinetics of nucleotide incorporation.

Structural Characterization of Motif D—The alignment of motif D from various RNA-dependent DNA polymerases is shown in Fig. 2*A*. Two amino acids are strictly conserved in this motif: Gly-213 and Lys-220, using HIV-1 RT amino acid numbering as a reference (16). To gain insight into the possible role of motif D, we took advantage of the observation that Pol I-type polymerases do not have an identifiable motif D. We have superimposed crystal structures of polymerases possessing a motif D, such as HIV-1 RT and MuMLV RT, onto those of Pol I-type polymerases that lack motif D, such as *Taq* DNA polymerase (7), Klenow fragment (8), and T7 DNA polymerase (9). The three conserved acidic amino acids located in the polymerase active site were chosen as anchoring points (3, 23). The result of this superimposition is shown in Fig. 3*A*. For clarity the only RT structure shown is HIV-1 RT (Protein Data Bank accession number 1RT1) (24), and it is compared with Pol I-type DNA polymerases cited above. The nucleotide ddGTP is taken from the ternary complex of T7 DNA polymerase-DNA-nucleotide together with two magnesium ions at the active site. Taking HIV-RT amino acid numbering as a reference, it can be seen that motif D contains a unique loop made of residues Thr-215 to Lys-223 protruding into the solvent. There is no structurally equivalent loop in Pol I-type polymerases (Fig. 3*A*). Lys-220 of RT is located at the tip of the loop facing the β3 and β4 strands. These strands are the structural equivalents of helix O of type I DNA polymerases. The corresponding helix of T7 DNA polymerase is shown together with the bound nucleotide ddGTP as seen in the structure of the T7 DNA polymerase complex (9).

During processive DNA synthesis by DNA polymerases, the rate-limiting step is a conformational change occurring from an "open" to a "closed" state before catalysis (18). In Fig. 3*A*, the β3 and β4 strands of RT are shown in the open conformation, and

A

Motif D	*Origin*	*Reference*
895...GCVVNLRKTVVN	*hTERT*	*(37)*
693...GFQKYNAKANRD	*yEST2*	*(37)*
252...GYRASAKKAQIC	*MuMLV*	*(34)*
214...GFSTPDEKFQKD	*HIV-2*	*(22)*
213...GLTTPDKKHQKE	*HIV-1*	*(16)*

B

Motif D variants of HIV-1 RT	*Name*	*Reference*
213...GLTTPDKKHQKE	*Wild-type*	*(16)*
...G------Q----	*K220Q*	*This study*
...G----N------	*D218N*	*This study*
...G-F---------	*T215F*	*(22)*
...G-F---Q-----	*T215F, K219Q*	*This study*
...G-F---Q-----	*D67N, K70R,T215F, K219*	*(22)*
...G-T_{215}VEVK$_{223}$ E	*Chimeric*	*This study*

FIG. 2. **Primary structure of motif D.** *A*, amino acid sequence alignments of various RNA-dependent polymerases. The number at the beginning of each line corresponds to the amino acid number of the first conserved glycine residue *underlined* in the sequence. *hTERT*, human telomerase catalytic subunit (37); *yEST2*, yeast telomerase catalytic subunit (37); *MuMLV*, murine Moloney leukemia virus reverse transcriptase (34); *HIV-2*, human immunodeficiency virus type 2 reverse transcriptase (22); *HIV-1*, human immunodeficiency virus type 1 reverse transcriptase (22). *B*, amino acid variants studied in this work. The *names* on the *right* correspond to the sequences shown on the *left*.

helix O of T7 is shown in the closed conformation. To define a potential role for motif D in the conformational change associated with nucleotide binding, the latter change was visualized by comparing two RT crystal structures (Fig. 3*B*). One RT (1RT1, pictured in *green*) has been crystallized in the absence of dNTP and nucleic acid and is thus interpreted to be in the open conformation (24). Lys-220 in the motif D loop points toward the Asp-67/Lys-70 finger tip region connecting β3 and β4 strands. The other RT (1RTD, pictured in *red*) has been crystallized in the presence of both dNTP and DNA and is thus in the closed conformation, which approximates the catalytic step (13). Lys-220 is pointing away from the Asp-67/Lys-70 region in this structure. However, its immediate neighbor Lys-219 can potentially make a salt bridge with Asp-67 in the 1RTD structure (see Fig. 4 in Ref. 13), whereas it is pointing away of Asp-67 in the structure of Esnouf *et al.* (24) (1RT1). B-factor values associated to atomic co-ordinates are higher than 50 Å^2 for α-carbons of residues Thr-215 to Lys-223 in both 1RT1 and 1RTD as well as in many published RT crystal structures, indicating that this region is rather flexible. Therefore, both Lys-220 and the motif D loop can adopt strikingly different conformations depending on the open or closed state of RT. Fig. 3*B* also shows that these two states might define a channel. To further document and examine the role of both this channel and the loop, we have generated RTs with various amino acid changes within motif D.

Amino Acid Substitutions in Motif D—We have engineered a series of RT genes to generate various amino acid changes in motif D as listed in Fig. 2*B*. Two of these enzymes have been characterized in detail. In one enzyme, the conserved Lys-220 was changed to glutamine to eliminate the positive charge of the ϵ-amino group while introducing minimal change in the length and polarity of the side chain. In the second enzyme, the Thr-215 to Lys-223 loop was eliminated and replaced by a segment of amino acids having the sequence T^{215}VEVK^{223}, corresponding to the shorter sequence present in *Taq* DNA polymerase (Fig. 3*A*). This peptidic fragment TVEV does not form a loop as seen in the *Taq* structure (Figs. 3*A*). This hybrid RT will be referred to as the "chimeric" RT.

Expression and Purification of RTs—The genetically altered RTs were overproduced in *E. coli* and purified as described under "Experimental Procedures." They were assayed for both reverse transcriptase and DNA polymerase activities. Only two of the RT variants modified in motif D showed a significant decrease of either polymerase activities. Using various template primer systems, RT(K220Q) and the chimeric RT had 3–8-fold and 50–2000-fold reduced polymerase activity compared with wild-type RT, respectively. One possible explanation was that both RT(K220Q) and the chimeric RT have a lower affinity for their template primer than does wild-type RT. Therefore, out of the various variant RTs shown in Fig. 2*B*, only wild-type RT, RT(K220Q), and the chimeric RT were used to compare their affinities for primed DNA or RNA templates.

Cross-linking of Template Primer to RT—The affinity of RT(K220Q) and the chimeric RT for a template primer was first examined relative to that of wild-type RT using a cross-linking assay. In this assay, a photo-reactive group is coupled to a 21-mer DNA primer at the 15th internucleotidic phosphate, taking the first nucleotide at the 3′-end of the primer as a reference (19). The 21-mer primer is labeled at the 5′-end using ^{32}P, annealed to a 31-mer DNA template, and RT is allowed to bind. The mixture is UV-irradiated, the products is separated on a denaturing polyacrylamide gel containing both SDS and 7 M urea, and radioactive signals corresponding to the primer attached to the p66 subunit are measured. As shown in Fig. 4*A*, no detectable difference in the amount of wild-type RT, RT(K220Q), and the chimeric RT cross-linked to primer was observed. When comparing the amount of two RT-cross-linked primer complexes on a gel, it is important to know how an observed difference between two complexes translates into a difference in affinity of RT for its template primer. Indeed, a very small difference in radioactive signals barely detectable in this assay could translate into a significant change in K_d of RT for its template primer. We calculated this theoretical difference as described under "Experimental Procedures," and the results are presented in Fig. 4*B*. According to the theoretical curve presented in Fig. 4*B*, a 2-fold increase of K_d value relative to wild-type (K_d = 5 nM) (17) would correspond to an 8% variation in the amount of radioactive signal measured on the gel. Because a 5% signal variation is readily detectable by this method and is not observed in Fig. 4*A*, we conclude that RT(K220Q) and chimeric RT bind duplex DNA with an affinity similar to that of wild-type RT.

Effect of Alteration of Motif D on the Affinity Constant K_d of RT for Template Primer—In another set of experiments, the K_d values for template primer were measured using

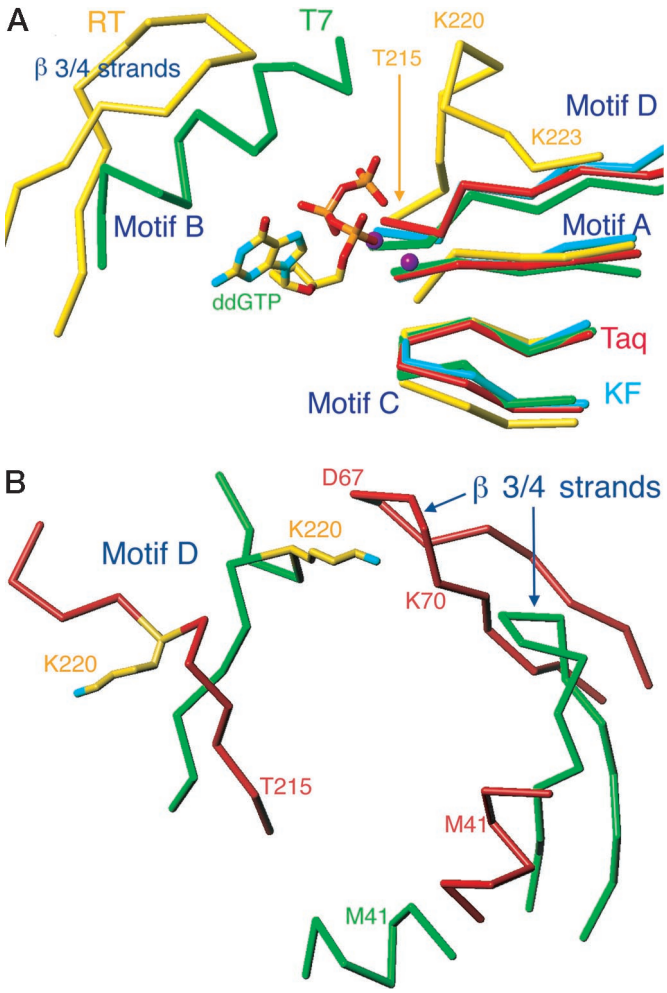

FIG. 3. **Structural alignments of RT and DNA polymerases of the type I family.** Atomic coordinates of RT, Klenow fragment (*KF*), *Taq* DNA polymerase (*Taq*), and T7 DNA polymerase (*T7*) were used to superimpose the corresponding crystal structures using the RIGID option of the TURBO graphics program. *A*, RT (1RT1, *yellow*) (24), Klenow fragment (1KFD, *blue*) (8), *Taq* (1TAQ, *red*) (7), and T7 DNA pol (1T7P, *green*) (9) crystal structures were superimposed using three catalytic acidic residues conserved in all polymerases (D110/D185/D186, D705/D882/E883, D610/D785/E786, and D475/D654/E655 for RT, Klenow fragment, *Taq*, and T7 DNA pol, respectively). The nucleotide ddGTP is taken from the ternary complex made of T7 DNA polymerase-DNA-nucleotide together with the two magnesium ions (shown as *purple spheres*) at the active site (9). The zones shown correspond to motifs A, B, C, and D as indicated. The orientation of the DNA (not shown) is from the *bottom right corner* to the nucleotide ddGTP. α-Carbons of Pol I-type polymerases in the vicinity of the α-carbon of Thr-215 of RT are Asp-691 for T7 DNA polymerase, Leu-915 for Klenow fragment, and Glu-817 for *Taq* DNA polymerase. Likewise, the α-carbon of Lys-223 of RT is in the vicinity of Gly-697 for T7 DNA polymerase, Gly-921 for Klenow fragment, and Gly-822 for *Taq* DNA polymerase. *B*, RT crystal structures (1RT1, shown in *green*, and 1RTD, shown in *red*) (13, 24) were superimposed as described above. The *green* structure corresponds to the open state, whereas the *red* corresponds to the closed conformation as described in the text and in Refs. 13 and 24. The view is approximately 180° relative to *panel A*. Part of the α-helix including M41 involved in AZT resistance is shown.

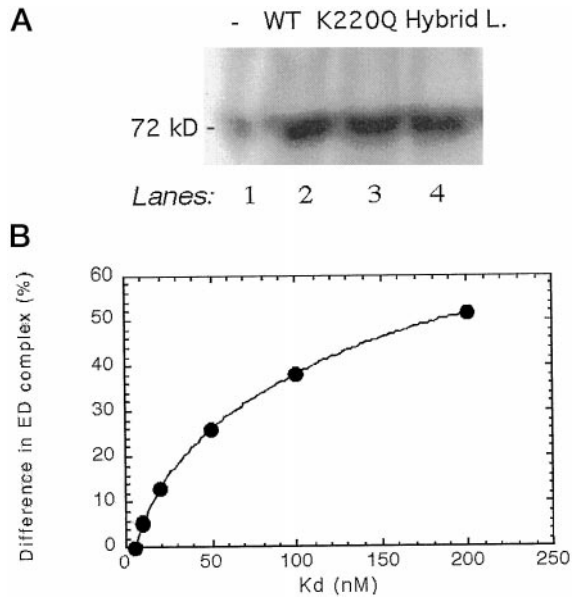

FIG. 4. **Affinity of wild-type RT, RT(K220Q), and chimeric RT for a template primer as determined by UV cross-linking.** *A*, electrophoretic analysis of the cross-linking products of wild-type, K220Q, and chimeric RT to a 5′-^{32}P-end labeled DNA primer containing a *p*-azidophenacyl photo-reactive group. Wild-type, K220Q, or chimeric RT (250 nM) was bound to a 5′-^{32}P-end labeled 21-mer DNA primer annealed to a 31-mer DNA template (250 nM) in RT buffer (see "Experimental Procedures"). The mixture was cross-linked under UV (365 nm) and subjected to denaturing gel electrophoresis containing both SDS and 7 M urea. The figure is an autoradiograph of the gel. The apparent molecular mass of the complex is indicated on the left. *Lane 1*, no RT; *lane 2*, wild-type RT; *lane 3*, RT(K220Q); *lane 4*, chimeric RT. *B*, theoretical variation of the amount of radioactivity present in cross-linking complex products such as those seen in *A* as a function of K_d of RT for the template primer. The reference point is wild-type RT (K_d = 5 nM) on the *x* axis (see text for details).

poly(rA)·oligo(dT)$_{19}$ and dTTP as a template primer system as described (25). No significant differences were found. For wild-type RT, RT(K220Q), and chimeric RT, the K_d values were equal to 2, 1, and 4 nM, respectively. We conclude that RT(K220Q) and the chimeric RT have the same affinity as wild-type RT for DNA primers annealed to DNA or RNA templates.

Processivity of DNA Synthesis—A change in processivity of nucleotide polymerization could potentially account for the difference in polymerase activity between wild-type RT, RT(K220Q), and the chimeric RT. Processivity of DNA synthesis is defined as the number of nucleotides incorporated during a cycle of polymerization prior to the dissociation of the polymerase from the nascent DNA strand. Processivity of nucleotide polymerization was assayed by first binding the RT to a 5′-labeled primer annealed to a homopolymeric template and initiating DNA synthesis by the addition of nucleotides. Heparin is added to serve as a trap for RT that dissociates during the reaction. A nonprocessive (distributive) enzyme will fall off the nascent DNA strand during polymerization and be caught in the trap, with a resulting decrease in product size (25). The processivity of wild-type RT, RT(K220Q), and chimeric RT was measured using a poly(rA)/5′-^{32}P-oligo(dT)$_{19}$ template primer. The absence of any synthesis when heparin was added prior to nucleotides indicated that the heparin trap was efficient (Fig. 5, *lane 1*). In the absence of the trap, wild-type RT incorporates more than 300 nucleotides within 1–5 min (*lanes 2* and *3*). The presence of the trap had no effect on the average size distribution of the product, indicating processive DNA synthesis (*lanes 4* and *5*). For both RT(K220Q) and the chimeric RT, DNA synthesis proceeded slower relative to wild-type RT (*lanes 2* and *3* in each case). However, the presence of the trap had no effect on the size distribution of the products (*lanes 4* and *5*). We conclude that neither the K220Q mutation nor the chimeric fragment in motif D affected the processivity of DNA synthesis. The results obtained here as well as in the previous section indicate that the apparent decrease in DNA polymerase activity of the chimeric RT relative to RT(K220Q) and wild-type RT is not due to an altered binding of RT to the template primer. To gain insight into the possible involvement of motif D into

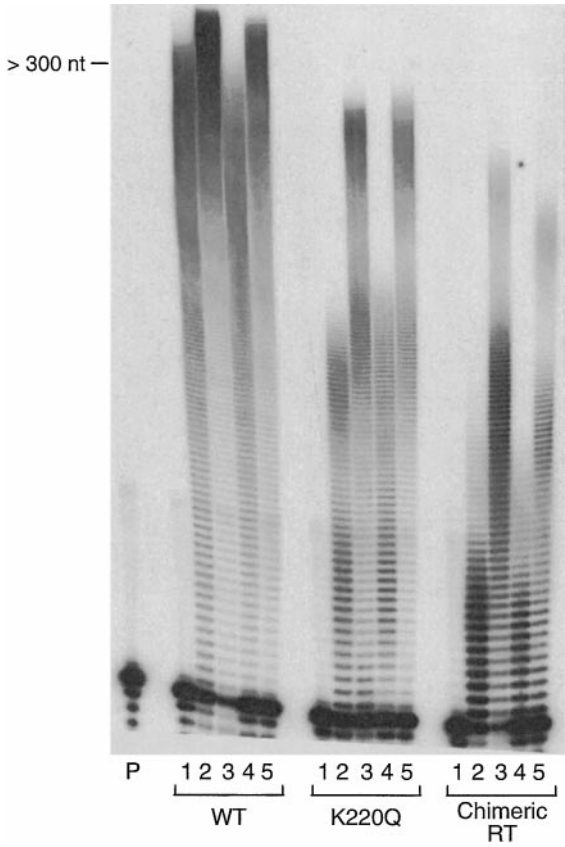

FIG. 5. **Processivity of nucleotide polymerization.** Polymerase activity of wild-type RT, RT(K220Q), and the chimeric RT was measured by primer extension on homopolymeric templates. Wild-type RT, RT(K220Q), or chimeric RT was bound to a 5′-^{32}P-end labeled oligo(dT)$_{19}$ primer annealed to a poly(rA) template as described under "Experimental Procedures." At time 0, 1 mM dTTP was added with or without 2 μg/μl heparin to serve as a trap for free RT. Effectiveness of the heparin trap was tested for each enzyme by incubating the enzyme with heparin before the addition of the poly(rA)·oligo(dT)$_{19}$ template primer (*lane 1*). DNA synthesis was initiated by the addition of dTTP alone and incubated for either 1 min (*lane 2*) or 5 min (*lane 3*). Processive DNA synthesis was measured by the addition of a mixture of dTTP and heparin trap and incubated for either 1 min (*lane 4*) or 5 min (*lane 5*). Aliquots were withdrawn, and the reaction quenched with an equal volume of gel loading buffer before being subjected to denaturing gel electrophoresis as described under "Experimental Procedures." The figure is an autoradiograph of the gel. The position of the unextended 5′-^{32}P-end labeled 19-mer oligo(dT) primer is indicated by *P*.

nucleotide selection, we examined the kinetics of nucleotide polymerization of wild-type RT, RT(K220Q), and the chimeric RT.

Steady-state Kinetics of RT(K220Q) and Chimeric RT—We have determined steady-state constants of wild-type RT, RT(K220Q), and chimeric RT prepared as p66/p66 homodimers. Because the other RT variants shown in Fig. 2*B* did not exhibit different kinetics of nucleotide polymerization relative to wild-type RT, their steady-state constants were not determined. Furthermore, steady-state parameters of the clinically relevant mutant RT(D67N/K70R/T215F/K219Q) p66/p66 homodimer have been studied in detail and found to be essentially the same as those of wild-type RT (26–28). The experiments were carried out using standard DNA primed homopolymeric RNA and DNA templates that specify incorporation of either dTTP, dGTP, or dATP. Results corresponding to the use of DNA templates are shown in Table I. Using poly(dA)·oligo(dT)$_{21}$ as template primer, RT(K220Q) had an affinity for dTTP comparable with that of wild-type RT, while the K_m(dTTP) for the chimeric RT increased 18-fold relative to wild-type RT. Both RT(K220Q) and chimeric RT had a 4-fold lower k_{cat} than wild-type RT. These values were used to calculate the overall efficiency of dTTP incorporation in terms of k_{cat}/K_m. RT(K220Q) and the chimeric RT had 8- and 86-fold decreased efficiency relative to wild-type RT, respectively. Very similar results were observed using poly(dC)·oligo(dG)$_{21}$ as template primer. RT(K220Q) had an affinity for dGTP similar to that observed for wild-type RT, but K_m(dGTP) for the chimeric RT increased nearly 10-fold. The k_{cat} values of K220Q and chimeric RT were comparable but 2–5-fold lower than that of wild-type RT. In summary, for DNA-dependent DNA synthesis, the K220Q substitution decreased the k_{cat} only about 2–5-fold, whereas the chimeric RT exhibited a 10–20-fold decrease in the affinity for dNTP, with no further decrease in k_{cat} relative to that found with RT(K220Q).

TABLE I
Steady-state kinetic constants of wild-type RT, RT(K220Q), and chimeric RT for primed homopolymeric DNA templates

	Poly(dA) · oligo(dT)$_{21}$			Poly(dC) · oligo(dG)$_{21}$		
	K_m (dTTP)[a]	k_{cat}[a]	k_{cat}/K_m	K_m (dGTP)[a]	k_{cat}[a]	k_{cat}/K_m
	μM	s^{-1}	$s^{-1}\cdot\mu M^{-1}$	μM	s^{-1}	$s^{-1}\cdot\mu M^{-1}$
Wild type	3.8	0.01	0.0026	3	0.33	0.11
K220Q	7.7	0.0025	0.00032	4.5	0.17	0.038
Chimeric	70	0.0021	0.00003	35.4	0.07	0.002

[a] Polymerase activity was measured using the filter paper assay described under "Experimental Procedures." K_m and k_{cat} were obtained using Eadie-Hofstee plots in which values of correlation coefficients were greater than 0.9.

These RTs were then assayed on homopolymeric RNA templates (Table II). The kinetic parameters followed the same pattern of alteration. For both poly(rA)·oligo(dT)$_{19}$ and poly(rC)·oligo(dG)$_{19}$ template primers, K_m(dNTP) was essentially identical for RT(K220Q) relative to wild-type RT while a 3–7-fold decrease in k_{cat} was observed. The chimeric RT showed a 26–220-fold increase in K_m with no further change in k_{cat} relative to RT(K220Q). Relative to wild-type RT, these changes in K_m and k_{cat} produced 3–5-fold and 115–2000-fold decreases in polymerization efficiency as judged by k_{cat}/K_m for RT(K220Q) and the chimeric RT, respectively (Table II).

To test whether this pattern of variation of K_m and k_{cat} was found for other nucleotides, the same steady-state kinetic experiments were also performed using poly(rU)·oligo(dA)$_{21}$ as a template primer system. Both the decrease in k_{cat} and the increase in K_m observed with other template primer systems were also found for RT(220Q) and the chimeric RT, respectively. RT(K220Q) had a 5-fold decreased efficiency relative to wild-type RT, whereas chimeric RT had a nearly 400-fold decreased efficiency, as judged by k_{cat}/K_m values (Table II).

We conclude that changes in motif D affect both nucleotide binding and catalysis, whereas the affinity for the template primer remains unchanged. The K220Q substitution has a modest effect on k_{cat}, and the deletion of the loop greatly decreases the affinity of the chimeric RT for the nucleotide substrate. The poor catalytic efficiency of the chimeric mutant RT is due to low nucleotide incorporation efficiencies on both DNA and RNA templates (k_{cat}/K_m; Tables I and II). To characterize how motif D interacts with the incoming nucleotide, we made use of nucleotide analogues in conjunction with RT variants altered in motif D.

Effect of Alterations in Motif D on Discrimination against Nucleotide Analogues—Two clinically important amino acid changes leading to drug resistance occur in motif D of HIV-1 RT. T215(F/Y) and K219Q substitutions are found in RT from AZT-resistant viruses when the nucleotide analogue AZT is used as a chemotherapeutic agent alone (22). AZTTP, the active form of AZT, is a thymine nucleotide differing from dTTP

TABLE II
Steady-state kinetic constants of wild-type RT, RT(K220Q), and chimeric RT for primed homopolymeric RNA template

	poly(rA)·oligo(dT)$_{19}$			poly(rC)·oligo(dG)$_{19}$			poly(rU)·oligo(dA)$_{21}$		
	K_m (dTT)[a]	k_{cat}[a]	k_{cat}/K_m	K_m (dGTP)[a]	k_{cat}[a]	k_{cat}/K_m	K_m (dATP)[a]	k_{cat}[a]	k_{cat}/K_m
	μM	s^{-1}	$s^{-1}\cdot\mu M^{-1}$	μM	s^{-1}	$s^{-1}\cdot\mu M^{-1}$	μM	s^{-1}	$s^{-1}\cdot\mu M^{-1}$
Wild type	5.8	2.4	0.42	7.6	1.75	0.23	6.8	0.85	0.125
K220Q	4.5	0.35	0.078	7.5	0.6	0.08	23.5	0.52	0.022
Chimeric	1120	0.21	0.00018	201	0.37	0.0018	523	0.17	0.00033

[a] Polymerase activity was measured using the filter paper assay described under "Experimental Procedures". K_m and k_{cat} were obtained using Eadie-Hofstee plots in which values of correlation coefficients were greater than 0.98.

only by the presence of an azido group at the 3′ position of the ribose. Hence, incorporation of AZTMP by RT in a growing DNA strand results in inhibition of polymerization as a result of chain termination (22). It was thus of interest to determine whether the 3′-group of a nucleotide interacts with motif D. Reverse transcriptase activity was measured using poly(rA)·oligo(dT)$_{19}$ in the presence of [H^3]dTTP as the sole nucleotide substrate. When increasing concentrations of AZTTP are added to the reaction, inhibition occurs because of chain termination. Because processivity of DNA synthesis of the wild-type RT, RT(K220Q), and the chimeric RT are comparable, this parameter should not alter the relative inhibition observed (29). K_i(AZTTP) of these three RTs was determined. Fig. 6 shows the inhibition plot using AZTTP for both RT(K220Q) and chimeric variants relative to wild-type RT. RT(K220Q), and the chimeric variant exhibited AZTTP resistance of 10- and 200-fold relative to wild-type RT as determined by the ratio of their K_i relative to that of wild-type RT, respectively. This discrimination was specific for a 3′-azido group. Indeed, the same experiment was performed using ddTTP instead of AZTTP, and similar results were obtained, although ddTTP is a less potent inhibitor of RT (30). There was no change in the order of increasing discrimination among various RT variants studied.

To confirm these results, a primer extension assay was performed in which RT incorporates dTTP in the presence of either AZTTP or ddTTP. A 5′-^{32}P-labeled oligo(dT)$_{19}$ primer is annealed to a poly(rA) template, and RT is allowed to bind. The reaction is initiated by the addition of dTTP in the presence of either AZTTP or ddTTP. As the variant RTs exhibited higher fold of discrimination for AZTTP and ddTTP, the reaction was incubated for 60 min instead of 5 min to allow maximum incorporation of the nucleotide analogues, thus allowing us to compare the wild-type and variant RTs. The products are analyzed using denaturing gel electrophoresis as described in the previous section for the processivity assay. Fig. 7 shows the result of such an experiment. In the absence of AZTTP, wild-type RT, RT(K220Q), and chimeric RT were able to extend the (dT)$_{19}$ primer by 300 nucleotides or more (*lanes 1–3* of the *left panel*). It should be noted that the extent of DNA synthesis in the absence of any inhibitor by all the RTs is higher that seen for the processivity experiment. This difference is due to the longer reaction time. In the presence of 100 μM AZTTP, inhibition of wild-type RT by chain termination became apparent as visualized by the presence of shorter extension products whose average size was approximately 15 nucleotides in length (*lane 1*, *middle panel*). In contrast to wild-type RT, RT(K220Q) and chimeric RT were able to extend the (dT)$_{19}$ primer approximately 200 nucleotides (*lane 2* and *3*, respectively, *middle panel*). When ddTTP was used as the inhibitor, wild-type RT exhibited sensitivity toward ddTTP although to a lesser extent than AZTTP (*lane 1*, *right panel*), whereas inhibition was hardly apparent for RT(K220Q) and chimeric RT (*lanes 2* and *3*, *right panel*). There was no difference in the extent of inhibition between RT(K220Q) and the chimeric RT using either inhibitor, but we did not attempt to optimize the assay to visualize the difference. Consistent with results obtained using the filter paper assay, AZTTP was a better inhibitor than ddTTP of wild-type RT, RT(K220Q), and chimeric RT. We conclude that the 3′-group of the incoming nucleotide is also interacting with amino acid(s) present in motif D at some point before or during incorporation into DNA.

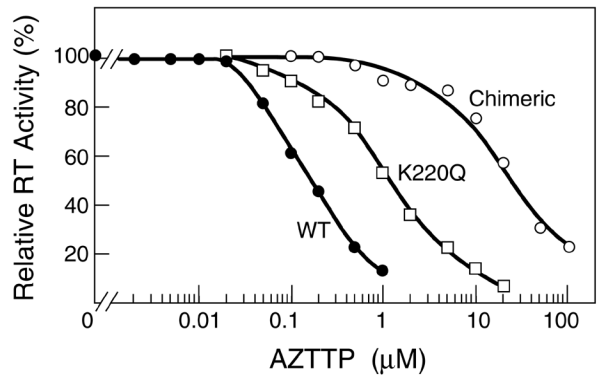

FIG. 6. **Effect of alterations in motif D on discrimination against AZTTP.** Wild-type, K220Q, or chimeric RT was incubated with poly(rA)·oligo(dT)$_{19}$ and [^{3}H]dTTP in RT buffer as described under "Experimental Procedures." AZTTP was present at various concentrations as indicated, and the polymerization rate was measured relative to the uninhibited reaction. For each RT, the AZTTP concentration producing 50% inhibition of the reaction (IC$_{50}$) was determined manually from the graph.

DISCUSSION

The replicative enzyme of HIV-1 is both an RNA- and DNA-dependent DNA polymerase. Like most RNA-directed polymerases RT contains in its palm region a conserved motif termed motif D (6). The recent crystal structure at 3.2 Å resolution of a ternary complex made of HIV-1 RT, template primer, and a nucleoside 5′-triphosphate has cast light on how RT interacts with its substrates (13). The structure shows that the single-stranded 5′-extension of the DNA template does not penetrate into the large cleft, avoiding both motif D and the fingers β3/β4 strands domain (Fig. 1). This finding corrects previous structural studies proposing that the template extension would penetrate into the cleft to potentially interact with motif D and β3/β4 strands. Consequently, it is unlikely that both β3/β4 strands and motif D of RT would be involved in template specificity. We have examined the role of motif D of HIV-1 RT and shown that amino acid changes within a loop located in motif D affect nucleotide selectivity but not template specificity.

We first conducted a structural study of motif D using the atomic coordinates of several crystal structures of RT in comparison with other DNA polymerases that do not have an identifiable motif D. Our study shows that motif D comprises a loop whose position is consistent with having an interaction with the incoming nucleotide. It can be seen in the structure of a RT-template primer-nucleotide complex that motif D can interact with the fingers domain of RT making a channel-like structure occluded by the DNA 3′-end (Fig. 1 and Ref. 13). The entrance of this channel can be seen in Fig. 3*B*. Upon binding of the

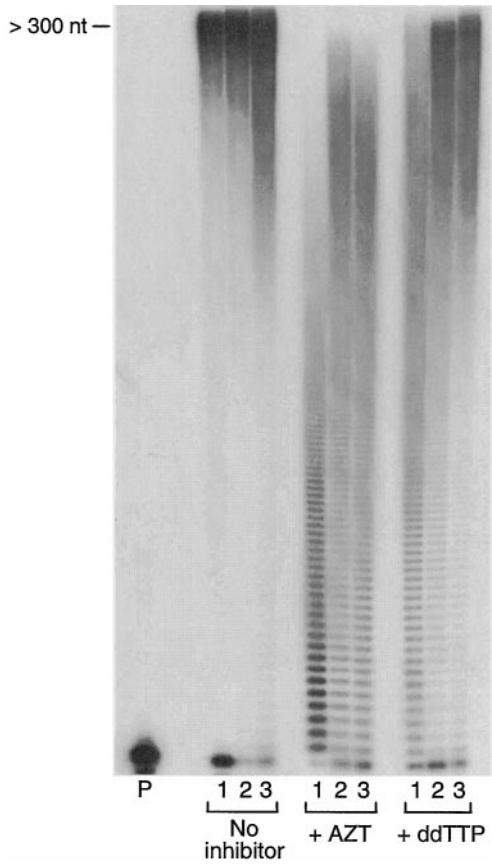

FIG. 7. **AZTTP/ddTTP discrimination using a primer extension assay.** The reaction mixture containing 100 nM 5′-^{32}P-end labeled 19-mer oligo dT primer annealed to poly(rA) in RT buffer and 1 mM dTTP (see "Experimental Procedures") was incubated with 50 nM of wild-type RT, RT(K220Q) or chimeric RT in the absence (*left panel*) or presence of 100 μM AZTTP (*middle panel*) or ddTTP (*right panel*) at 37 °C and incubated for 60 min. The reaction products were analyzed using denaturing gel electrophoresis. The figure is an autoradiograph of the gel. *Lane P*, 19-mer oligo dT primer alone; *lanes 1*, *2*, and *3*, in each panel represent wild-type RT, RT(K220Q), and chimeric RT, respectively.

dNTP substrate, a large movement of both fingers and motif D domains occurs, greatly modifying the topology of the putative nucleotide channel (Fig. 3*B*). The most conserved residues Gly-213 and Lys-220 of motif D are located upstream and at the tip of the motif D loop, respectively. Glycine residues often provide flexibility to a peptide chain. Therefore, Gly-213 might provide a hinge for the loop with Lys-220 having a role in its mobility.

Based on this model, we modified the amino acid sequence of motif D using site-directed mutagenesis. RT genes corresponding to clinically relevant mutants such as T215F, T215F/K219Q, and D67N/K70R/T215F/K219Q were constructed. RT genes were also constructed in which charged amino acid residues such as Asp-218 and Lys-220 were replaced with uncharged residues (Fig. 2*B*). Indeed, examination of the crystal structure of RT indicated that the charged amino acids of motif D loop could potentially interact with residues present in the β3/β4 strands of RT (Fig. 3*B*). The loop was also eliminated and replaced by a segment of shorter sequence present in *Taq* DNA polymerase to generate what we have designated as chimeric RT. The corresponding variant RTs were purified and studied for their template binding properties and kinetics of nucleotide incorporation.

RT having D218N, T215F, T215F/K219Q, or D67N/K70R/T215F/K219Q substitutions did not exhibit any obvious phenotype as judged by their unaltered polymerase activity. In contrast, the RT(K220Q) and the chimeric RT exhibit a decreased polymerase activity that was not due to decreased template primer binding. Rather, this decreased activity could be attributed to a modest effect on k_{cat} of RT(K220Q) and a dramatic effect on K_m(dNTP) for the chimeric RT. Therefore, it is clear that the loop in motif D of RT is mainly involved in nucleotide binding.

Surprisingly, however, the K220Q substitution produces a 10-fold discrimination against AZTTP relative to wild-type RT. This effect is most likely due to a favorable interaction of the correct 3′-ribose through direct interaction of the ϵ-amino group of Lys-220 with the 3′-OH of the incoming nucleotide. Indeed, discrimination of ddTTP is also increased using the K220Q variant, indicating that steric hindrance brought by the 3′-azido group is not relevant. One possible scenario for nucleotide incorporation is that initial binding of the nucleotide occurs within the lysine-rich β3/β4 fingers domain through the triphosphate moiety in a base-independent process as previously proposed (11, 31). Then, Lys-220 interacts with the 3′-OH of the nucleotide transiently during the conformational change preceding catalysis (18). In this scenario, Lys-220 and motif D would be required to allow the use of AZTTP as a substrate for reverse transcriptases. Consistent with this interpretation, deletion of the motif D loop affects nucleotide binding, catalysis, and promotes a 200-fold AZTTP discrimination relative to dTTP. This discrimination is consistent with AZTTP being a poor substrate for type I and eukaryotic DNA polymerases that do not have motif D and discriminate against AZTTP >100-fold relative to dTTP (32). The presence of K220Q in RT has been reported in one HIV-1 isolate (GenBank™ accession number U68954). Interestingly, the substitution K220Q occurs in this isolate together with L210W and T215Y, two amino acid changes implicated in AZT resistance (33).

Our results are also consistent with the classification of AZT resistance mutations by Huang *et al.* (13). These authors have pointed out that nucleoside analogue resistance mutations can be viewed as "rear" and "front" of the dNTP binding pocket. Using their terminology, we propose that rear mutations (such as M41L; Fig. 3*B*) located at the entrance of the dNTP channel might promote "sieving" of the nucleotide at the entrance of the channel. Lys-220 would be a residue participating in this process. The low k_{cat} of RT(K220Q) relative to wild-type RT might explain why mutations seldom involve K220Q in RT isolated from patients receiving AZT. On the other hand, front mutations (such as M184V) located at the bottom of the nucleotide channel would influence the catalytic step once the nucleotide has penetrated into the channel and closure of the fingers has taken place. Interestingly, MuMLV-RT discriminates to a greater extent than HIV-1 RT against ddNTPs. In the crystal structure of MuMLV RT, motif D loop is smaller in size and packed differently than the corresponding HIV RT loop (34). The proposition that motif D would be part of a nucleotide channel is consistent with the results of Patra *et al.* (35) who found that mutation of Phe-882 in motif D of T7 RNA polymerase leads to greater K_m for purines than pyrimidines (15). Finally, this proposition is also important to understand nucleoside analogue drug resistance. Positions of five clinically relevant amino acid changes (M41L, D67N, K70R, T215(F/Y), and K219Q) involved in AZT resistance are distributed on the circumference of the postulated nucleotide channel. Some of these amino acid changes are involved in the binding of the AZTMP-terminated primer by RT to enhance pyrophosphorolytic repair of the primer (17, 36). Like nucleotides, pyrophosphate should exit and enter toward the AZTMP-terminated primer through the nucleotide channel.

Acknowledgments—We thank Luis Menendez-Arias for drawing our attention to the U68954 Genbank sequence, and Luis Menendez-Arias, Nathalie Declerck, David Frick, and Lisa Rezende for critical reading of

the manuscript. We are extremely grateful to Patricia Hidalgo and Michael Sawaya for help with Fig. 1.

REFERENCES

1. Delarue, M., Poch, O., Tordo, N., Moras, D., and Argos, P. (1990) *Protein Eng.* **3,** 461–467
2. Braithwaite, D. K., and Ito, J. (1993) *Nucleic Acids Res.* **21,** 787–802
3. Steitz, T. A., Smerdon, S. J., Jager, J., and Joyce, C. M. (1994) *Science* **266,** 2022–2025
4. Joyce, C. M., and Steitz, T. A. (1994) *Annu. Rev. Biochem.* **63,** 777–822
5. Ollis, D. L., Brick, P., Hamlin, R., Xuong, N. G., and Steitz, T. A. (1985) *Nature* **313,** 762–766
6. Sousa, R. (1996) *Trends Biochem. Sci.* **21,** 186–190
7. Eom, S. H., Wang, J., and Steitz, T. A. (1996) *Nature* **382,** 278–281
8. Beese, L. S., Derbyshire, V., and Steitz, T. A. (1993) *Science* **260,** 352–355
9. Doublié, S., Tabor, S., Long, A. M., Richardson, C. C., and Ellenberger, T. (1998) *Nature* **391,** 251–258
10. Tantillo, C., Ding, J., Jacobo-Molina, A., Nanni, R. G., Boyer, P. L., Hughes, S. H., Pauwels, R., Andries, K., Janssen, P. A., and Arnold, E. (1994) *J. Mol. Biol.* **243,** 369–387
11. Wu, J., Amandoron, E., Li, X., Wainberg, M. A., and Parniak, M. A. (1993) *J. Biol. Chem.* **268,** 9980–9985
12. Boyer, P. L., Tantillo, C., Jacobo-Molina, A., Nanni, R. G., Ding, J., Arnold, E., and Hughes, S. H. (1994) *Proc. Natl. Acad. Sci. U. S. A.* **91,** 4882–4886
13. Huang, H., Chopra, R., Verdine, G. L., and Harrison, S. C. (1998) *Science* **282,** 1669–1675
14. Li, Y., Korolev, S., and Waksman, G. (1998) *EMBO J.* **17,** 7514–7525
15. Sousa, R., Chung, Y. J., Rose, J. P., and Wang, B. C. (1993) *Nature* **364,** 593–599
16. Larder, B. A., Purifoy, D., Powell, K. L., and Darby, G. K. (1987) *EMBO J.* **6,** 3133–3137
17. Canard, B., Sarfati, S. R., and Richardson, C. C. (1998) *J. Biol. Chem.* **273,** 14596–14604
18. Kati, W. M., Johnson, K. A., Jerva, L. F., and Anderson, K. S. (1992) *J. Biol. Chem.* **267,** 25988–25997
19. Canard, B., Sarfati, R., and Richardson, C. C. (1997) *Proc. Natl. Acad. Sci. U. S. A.* **94,** 11279–11284
20. Carroll, S. S., Geib, J., Olsen, D. B., Stahlhut, M., Shafer, J. A., and Kuo, L. C. (1994) *Biochemistry* **33,** 2113–2120
21. Roussel, A., and Cambillau, C. (1991) in *Silicon Graphics Directory*, p. 97, Silicon Graphics, Mountain View, CA
22. Larder, B. (1992) in *Reverse Transcriptase* (Skalka, A. M., and Goff, S. P., eds) pp. 205–222, CSHL Press, town, state
23. Yadav, P. N., Yadav, J. S., Arnold, E., and Modak, M. J. (1994) *J. Biol. Chem.* **269,** 716–720
24. Esnouf, R., Ren, J., Ross, C., Jones, Y., Stammers, D., and Stuart, D. (1995) *Nat. Struct. Biol.* **2,** 303–308
25. Huber, H. E., McCoy, J. M., Seehra, J. S., and Richardson, C. C. (1989) *J. Biol. Chem.* **264,** 4669–4678
26. Lacey, S. F., Reardon, J. E., Furfine, E. S., Kunkel, T. A., Bebenek, K., Eckert, K. A., Kemp, S. D., and Larder, B. A. (1992) *J. Biol. Chem.* **267,** 15789–15794
27. Kerr, S. G., and Anderson, K. S. (1997) *Biochemistry* **36,** 14064–14070
28. Krebs, R., Immendorfer, U., Thrall, S. H., Wohrl, B. M., and Goody, R. S. (1997) *Biochemistry* **36,** 10292–10300
29. Reardon, J. E., and Miller, W. H. (1990) *J. Biol. Chem.* **265,** 20302–20307
30. Reardon, J. E. (1992) *Biochemistry* **31,** 4473–4479
31. Painter, G. R., Wright, L. L., Hopkins, S., and Furman, P. A. (1991) *J. Biol. Chem.* **266,** 19362–19368
32. Cheng, Y. C., Dutschman, G. E., Bastow, K. F., Sarngadharan, M. G., and Ting, R. Y. (1987) *J. Biol. Chem.* **262,** 2187–2189
33. Harrigan, P. R., Kinghorn, I., Bloor, S., Kemp, S. D., Najera, I., Kohli, A., and Larder, B. A. (1996) *J. Virol.* **70,** 5930–5934
34. Georgiadis, M. M., Jessen, S. M., Ogata, C. M., Telesnitsky, A., Goff, S. P., and Hendrickson, W. A. (1995) *Structure* **3,** 879–892
35. Patra, D., Lafer, E. M., and Sousa, R. (1992) *J. Mol. Biol.* **224,** 307–318
36. Arion, D., Kaushik, N., McCormick, S., Borkow, G., and Parniak, M. A. (1998) *Biochemistry* **37,** 15908–15918
37. Counter, C. M., Meyerson, M., Eaton, E. N., Ellisen, L. W., Caddle, S. D., Haber, D. A., and Weinberg, R. A. (1998) *Oncogene* **16,** 1217–1222

The Motif D Loop of Human Immunodeficiency Virus Type 1 Reverse Transcriptase Is Critical for Nucleoside 5′-Triphosphate Selectivity

Bruno Canard, Kajal Chowdhury, Robert Sarfati, Sylvie Doublié and Charles C. Richardson

J. Biol. Chem. 1999, 274:35768-35776.
doi: 10.1074/jbc.274.50.35768